Soft Matter

Accepted Manuscript

This is an *Accepted Manuscript*, which has been through the Royal Society of Chemistry peer review process and has been accepted for publication.

Accepted Manuscripts are published online shortly after acceptance, before technical editing, formatting and proof reading. Using this free service, authors can make their results available to the community, in citable form, before we publish the edited article. We will replace this *Accepted Manuscript* with the edited and formatted *Advance Article* as soon as it is available.

You can find more information about *Accepted Manuscripts* in the Information for Authors.

Please note that technical editing may introduce minor changes to the text and/or graphics, which may alter content. The journal's standard Terms & Conditions and the Ethical guidelines still apply. In no event shall the Royal Society of Chemistry be held responsible for any errors or omissions in this *Accepted Manuscript* or any consequences arising from the use of any information it contains.

ROYAL SOCIETY OF CHEMISTRY

www.rsc.org/softmatter

Journal Name

RSCPublishing

ARTICLE

Solvent induced helical aggregation in the self-assembly of cholesterol tailed platinum complexes

Cite this: DOI: 10.1039/xoxxoooooox

Yueyuan Mao, Keyin Liu, Luyan Meng, Liang Chen, Liming Chen and Tao Yi*[a]

Received ooth January 2012,
Accepted ooth January 2012

DOI: 10.1039/xoxxoooooox

www.rsc.org/

Three alkynylplatinum (II) bipyridyl complexes in which two cholesterol groups are combined with a bipyridyl group via alkyl chains and amido bonds were designed and synthesized. The complexes have different lengths of ethylene glycol chains at the para-position of 1-phenylethyne. All three complexes can self-assemble to gel networks in DMSO, while only the morphology of **1a** without an ether chain shows well-defined right-handed helical structures with layer packing mode. However, **1c** with long ethylene glycol chains forms perfect regular left-handed helical structures in aqueous ethanol solution while the volume percentage of water is less than 5% (v/v). As the ratio of water increases, the chirality changes from a left-handed helix to a right-handed helix and the packing mode alters from the monolayer structure to the hexagonal structure. As the ratio of water further increases to greater than 50% (v/v), the structure of the assembly finally transforms to bilayer vesicles. The process of the morphology transition is traced by circular dichroism spectra, powder X-ray diffraction, SEM and TEM images. The result indicates that a polar solvent (water) acts as a trigger to change the self-assembly of the chiral structures of the complex due to the strong hydrophobic interaction between cholesterol groups and the balance of the hydrophobicity and hydrophilicity of the solvent environment.

Introduction

The construction of artificial helical polymers and supramolecular helical assemblies with controlled helicity has attracted significant interest in recent years in the fields of supramolecular chemistry and materials science because of their possible applications in molecular recognition, the separation of enantiomers, asymmetric catalysis and chiroptical devices.[1] Currently, many researchers focus on the helical structures and hope to selectively synthesize, induce or control the formation of the helical structure. Helical bundles or fibrils have been realized in synthetic proteins and peptides, [2] but a well-organized clear helix formed by synthetic organic molecules is still rare. The formation condition of the helical structures is rigorous, and the precise control of supramolecular helical architecture is a particularly important challenge in the field of molecular self-assembly.[3] Those self-assembled helixes are much more sensitive to outside stimuli, and their helical structures may be tuned by external forces including temperature,[4-6] light, [7-10] solvents (the constituent[11-16] and the chirality[17]), additives,[18-23] concentration,[24] coulombic repulsive interactions,[25] enantiomeric purity,[26] chiral memory introduced by a chiral "sergeant"[27] and isotopic substitution[28] and by the delicate balance of non-covalent forces. For example, Wei et al. found that the steric hindrance of substituent group and chiral dopants can induce the morphology transition of helical structures[19, 20, 29] which are formed via the polymerization of aniline or aniline derivative. Ajayaghosh et al. reported a helical unfolding and refolding mediated via cation[22] and a two-component multiple H-bonding self-assembly induced by the complementary guest.[21] A water-induced supramolecular charity inversion of a helical rosette nanotube in a G-C motif was reported recently in which the hydrogen bonds between the G and C motifs are the main driving force for the formation of the nanotube, and the percentage of water in the mixed solvent affects the chirality of the helical direction of the rosette nanotube.[12]

Cholesterols are important building blocks not only in biological systems but also in artificial self-assembly systems. The hydrophobic interactions of the cholesteric group contribute greatly to the self-assembling behaviors.[30-37] The chirality of carbon atoms and their ethylenic bonds have a great influence on their gelation ability and the state of aggregation structure in solvent.[30, 38-43] We have conducted some research on the effect of ultrasound on self-assembly properties such as morphologies, surface wettability, aggregated emission and reversible properties in a series of cholesteric derivatives.[32-36, 44, 45] As one of the most effective hydrophobic chiral function groups, cholesteric groups played an important role in the formation of some self-assembled chiral structures in which the gel phase was CD-active and the sol-gel transition was "read-out" as a change in CD spectroscopy.[31]

Soft Matter Accepted Manuscript

Organometallic platinum (II) complexes containing bipyridyl and alkynyl ligands are good skeletons for supramolecular assembly due to their intrinsic character, such as the intermolecular interactions of π-π stacking between the square planar bipyridyl ligand and the aryl alkynyl ligand, and the possible metal–metal interactions between the d8 metals.[46-51] Those platinum complexes already exhibited tremendous applications in the areas of catalysis,[52] anti-cancer drugs,[53] sensing applications[54] and stimulus-responsive self-assemblies. Despite the development of metallogels and chiral gelators, there is a lack of data on platinum complexes that form well-organized helical structures. Only alkynylplatinum (II) terpyridyl complexes with chiral groups [49] or bulk substituent groups[46] at the terpyridyl side were reported to self-assemble into helical nanofibers with steric hindrance as the driving force.

Herein, three alkynylplatinum (II) bipyridyl complexes in which two cholesterol groups are combined with a bipyridyl group via alkyl chains and amido bonds are designed (**1a-1c** in Scheme 1). The difference in these three complexes is the length of the ethylene glycol chains in the para-position of 1-phenylethyne. Thus, the platinum atom and the extended conjugated system are posited at the center of the molecules, while the balance of the hydrophobicity and hydrophilicity can be tuned by the length of the ethylene glycol chains. In addition, the ethylene glycol chains with different lengths on the phenylethyne fragment can modulate the solubility and amphiphilicity of the complex in protonic solvent. Thus, we speculate that the molecular chirality of the cholesterol group can be transferred into macro supramolecular chirality in these complexes through self-assemble processes via the hydrophobic interaction of the cholesteric group and π-π stacking of the central conjugated part; additionally, the subtle structure of the self-assembly may be dynamically tuned by modification of the hydrophobicity and hydrophilicity balance. The results show that all three complexes (**1a-1c**) can self-assemble to gels in DMSO, while only the morphology of **1a** gives well-defined right-handed helical structure. However, a chirality and morphology variation from a left-handed helix to a right-handed helix and vesicles are observed in **1c** with long ethylene glycol chains in a mixed solvent of water/ethanol as the volume ratio of water changes, accompanied by packing mode changes from a monolayer lamellar structure to a bilayer structure with a mesophase of hexagonal structure.

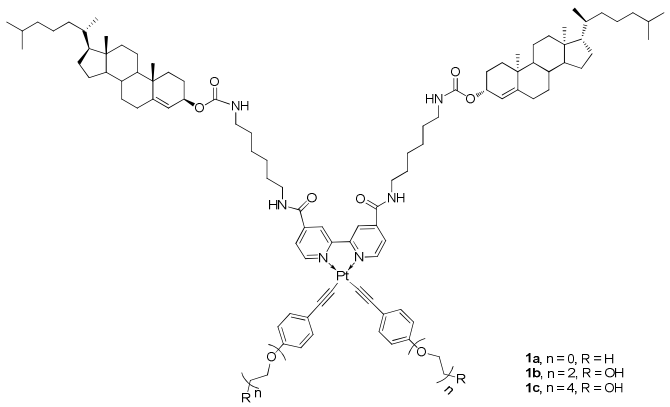

Scheme 1 The chemical structure of complexes **1a**, **1b** and **1c**.

Experimental procedure

Materials

All starting materials were obtained from commercial suppliers and were used as received. Cholesteryl chloroformate (99%) was obtained from Acros. Hexamethylene diamine and 2,2'-bipyridine-4,4'-dicarboxylic acid were supplied from Sinopharm Chemical Reagent Co., Ltd. (Shanghai). K_2PtCl_4 was provided from Accela ChemBio Co., Ltd. (Shanghai). Phenylacetylene (98%), ethylene glycol (99.5%), diethylene glycol (99%) and tetraethylene glycol (99.2%) were obtained from J&K Scientific Ltd.

Physical measurements and instrumentation

^{1}H NMR (400 MHz) and ^{13}C NMR (100 MHz) were recorded on a JEOL instrument (JEOL, Japan). Proton chemical shifts are reported in parts per million downfield from tetramethylsilane (TMS). ESI-MS data were recorded on a Micro TOF II 10257 Instrument (Bruker Daltonics Inc., Germany). Melting points were recorded on a WRS-2 microcomputer melting point meter without correction (China). SEM images were obtained with the help of an FE-SEM S-4800 (Hitachi) instrument. Samples were prepared by spinning the samples on mica slices and coating with Au. TEM images were recorded on a JEM -2100F. The samples were prepared by coating the diluted wet gels on a copper grid at room temperature and freeze drying (EYELA, FDU-1200) for 24 h. The XRD data were recorded on a D8 ADVANCE and a DAVINCI.DESIGN (Bruker Company, Germany). The SAXS were recorded on a NanoStar U SAXS System (Bruker Company, Germany). UV–visible absorption spectra were recorded on a Shimadzu UV-2250 spectrophotometer. Fluorescence spectra were recorded on an Edinburgh FLS-920 spectrophotometer (Germany) and circular dichroism spectra were recorded on a Bio-Logic MOS-450 CD instrument (Bio-Logic, France). Particle size distribution was studied by Malvern Zeta Sizer Nano Series, Nanosizer ZS90 and Malvern Autosizer4700.

Preparation method of the gels

The gels of **1a**, **1b** and **1c** in DMSO were made by the following method: When 10 mg of **1a**, **1b** or **1c** was added to 0.4 mL of DMSO, most of the gelator behaved as a precipitate. The mixture was changed into a transparent sol when heated. The transparent sol was changed into a gel after cooling at room temperature. Qualitatively, gelation was considered successful if no sample flow was observed upon inverting the container at room temperature. The critical gel concentration (CGC) was measured with the following method: 50 μL of additional DMSO was added into the above gel. The mixture was heated until the solid was dissolved and then cooled to room temperature and aged for a few minutes. If the gel was formed, the above procedures were repeated until the gel was collapsed. This concentration was determined to be the CGC. The gel-to-sol transition temperature (Tg) was tested with the

Soft Matter Accepted Manuscript

 This journal is © The Royal Society of Chemistry 2012

following method: The gel was put into a water bath, and the temperature of the water bath was increased gradually and was monitored with a thermometer. *T*g was the temperature when the gel collapsed.

The preparation of solution of 1b and 1c in water/ethanol

Firstly, **1b** and **1c** was dissolved in ethanol (2.0×10^{-4} mol·L^{-1}, 10 mL) to form prepared solution, respectively. Then 0.5 mL as prepared solution was added into a sample bottle with pipette, and all samples were diluted in to 1.0×10^{-4} mol·L^{-1} with water and ethanol to get the solution of **1c** in water/ethanol solution with various r_{aq} (r_{aq} is the volume percentage of water in water/ethanol solution). Then the samples were heated to 70~75°C and cooled to 20°C.

Results and discussion

The gelation properties of 1a-1c in DMSO

The gelation tests of the three complexes are carried out with various solvents by using a tube-inversion method.[55] The solubility and gelation properties of these three complexes are shown in Table 1. All three complexes are soluble in aprotic solvents, such as dichloromethane, chloroform, THF and toluene, but precipitate in protonic solvent at the concentration of 25 mg·mL^{-1} and are nearly insoluble in water. However, all of these complexes can gel DMSO with the CGC of **1a-1c** being 25, 8.3 and 16.7 mg·mL^{-1}, respectively. In addition, **1a** can also gel in cyclohexane. The gel to solvent transition temperature (*Tg*) of **1a-1c** in DMSO at the concentration of 25 mg·mL^{-1} is 42, 49 and 50 °C, respectively, which indicates that the thermal stability of the gels is increased with an increase in the ether chain length. In addition, the DMSO gel of **1b** and **1c** can stay at least 1 week at room temperature, much longer than that of **1a** (less than 2 days), which also indicates that the stability of the gels increases from **1a** to **1c**, in accordance with the changes in the *Tg* value.

Table 1. Solubility and gelation properties of **1a - 1c**.[a]

Solvent	**1a**[b]	**1b**[b]	**1c**[b]
Dichloromethane	S	S	S
Chloroform	S	S	S
Toluene	S	S	S
THF	S	S	S
Ethyl acetate	P	P	P
H_2O	I	PS	PS
Methanol	P	P	P
Ethanol	I	P	P
Isopropanol	P	P	P
N-Propanol	P	P	P
n-Butyl alcohol	P	P	S
DMSO	G (25)[c]	G (8.3)	G (16.7)
Cyclohexane	G (9.1)	P	P

[a] S = solution at room tempreture; G = gel; P = precipitate; I = insoluble; PS = partial soluble. The CGC of the gelators are given in parentheses [mg mL^{-1}]. [b] Heated to dissolve, cooled to room temperature, and aged for 30 min at the concentration of 25 mg·mL^{-1}. [c] The transparent sol first changes to an opaque sol at a concentration of 5 mg mL^{-1} and finally transfers to a gel at a concentration of 25 mg/mL^{-1}.

To investigate the self-assembly characteristics of the complexes in the gel state, the morphology of the three gels in DMSO is characterized by scanning and transmission electron microscopy (SEM and TEM). Interestingly, **1a** can form a well-organized right-handed helical structure from the SEM image (Fig. 1a). The lengths of the helical bands are in the range of several microns to tens of microns. Most of the helixes are intertexture to double or multi-helix, as shown in the SEM image, while single or double helical ribbons were clearly observed in the TEM image of a diluted gel sample (Fig. 1b and Fig. S1 in the ESI†). The helix is very uniform in both the SEM and TEM images, with a width of 20 nm and a screw-pitch of 65 nm (Fig. 1b, inset). The thickness of the helical ribbon is approximately 4.5 nm, which is approximately the length of two molecules (Fig. S2). The other two complexes with ethylene glycol chains form curly ribbon structures without clear helicity (Fig. 1c and 1d).

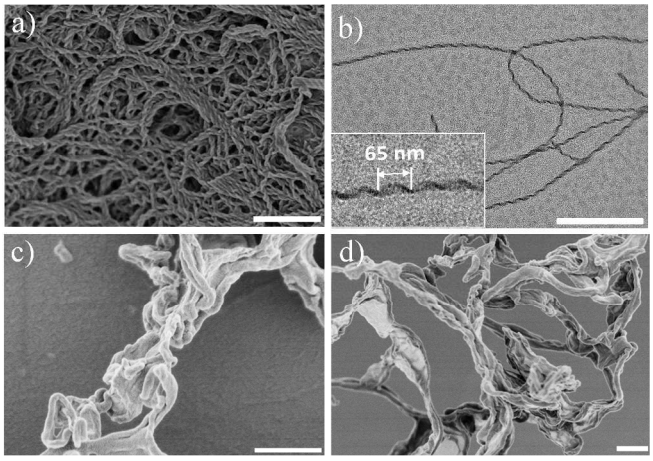

Fig. 1 SEM images of the xerogel of (a) **1a**, (c) **1b** and (d) **1c** (samples are shown in light colour); and (b) the TEM image of **1a** (samples are shown in dark colour). The scale bar is 500 nm. The inset in (b) shows an enlarged helix.

The helical structure of the **1a** gel was further confirmed by UV-visible absorption and circular dichroism spectra. All of the complexes have a strong absorption at approximately 296 nm in DMSO solution at the concentration of 1.0×10^{-5} mol·L^{-1} (Fig. 2a), which can be assigned to the intraligand (IL) [π-π*] transitions of bipyridine and alkynyl ligands, whereas the low-energy, moderately intense absorption bands at approximately 423 nm for **1a** and 445 nm for **1b** and **1c** are tentatively assigned as an admixture of metal-to-ligand charge transfer (MLCT) [dπ(Pt)-π*(bpy)] and ligand-to-ligand charge transfer (LLCT) [π(alkynyl)-π*(bpy)] transitions.[56] The red shift of the absorption bands of **1b** and **1c** in the visible range compared to **1a** is due to the electron-donating character of the ethylene glycol chains on the alkyl fragment of **1b** and **1c**. The absorption spectra of **1a-1c** in DMSO gels were also tested (the width of the cell is 0.1 mm). The absorption peak of **1a** was red shifted approximately 25 nm from the solution (1.0×10^{-5} mol·L^{-1}) to the gel state (40 mg·mL^{-1}, 2.41×10^{-2} mol L^{-1}), while the absorption of **1b** and **1c** shows no shift. This indicates that the π-π stacking interaction only exists in the self-assembly of **1a**, while **1b** and **1c** have different packing modes (Fig. 2b). The CD spectra of the gels of **1a-1c** in DMSO show that only the gel of **1a** produces a

Soft Matter Accepted Manuscript

strong negative Cotton effect at 274 nm and a weak negative Cotton effect at approximately 465 nm, while the other two gels show no obvious CD signals (Fig. 2c). The negative Cotton effect in gel **1a** is due to the π system chirality induced by the cholesterol groups, which is in accordance with the helical structure shown in the SEM images. The CD spectral of the **1a** gel in different diluted concentration showed that the intensity of the CD signal decreased with the decrease of the concentration, whereas the direction of the chirality had no change (Fig. S3). This result indicates π-π stacking between the central alkynyl platinum (II) bipyridyl part along the backbone of the aggregated cholesterol groups in **1a** gel.

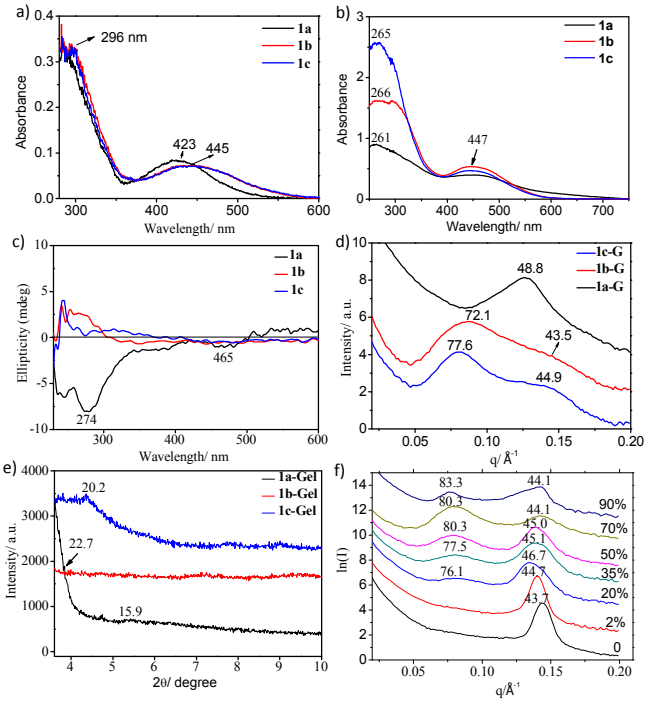

Fig 2. (a) The absorption spectra of the solutions of **1a**-**1c** in DMSO in the concentration of 1.0×10^{-5} mol·L^{-1}. (b) The absorption spectra of the gels of **1a**-**1c** in DMSO in the concentration of 40 mg·mL^{-1} (2.41×10^{-2} mol L^{-1}, 0.1 mm cell). (c) The CD spectrum of the gel of **1a** in DMSO (25 mg·mL^{-1}, 1.50×10^{-2} mol L^{-1}). (d) The SAXS patterns of the xerogel of **1a**-**1c** in DMSO; (e) the XRD of the xerogel of **1a, 1b and 1c** in DMSO; f) the SAXS of the precipitation of **1c** in water/ethanol with different r_{aq}. The numbers in the figures indicate the *d* value (Å)

To further study the self-assembly behaviors of these complexes, molecular packing of the **1a-1c** xerogels in DMSO is investigated by small angle X-ray scattering (SAXS) and powder X-ray diffraction (XRD). The SAXS patterns of the **1a-1c** xerogels from DMSO are tested and shown in Fig. 2d. Only one peak corresponding to the *d* value of 48.8 Å is observed in the SAXS pattern of **1a**, while in the larger angle area of the XRD spectra, two weak signals corresponding to *d* values of 22.7 and 15.9 Å (Fig. 2e) are observed. The three values produced a ratio close to 1: 1/2: 1/3, indicating the formation of lamellar structure in the helical ribbon of **1a**. The value of 48.8 Å is close to twice the length of a **1a** molecule, indicating that the lamellar structure is formed by a double layer of **1a** molecules. The SAXS pattern of **1b** and **1c** produced two peaks corresponding to the *d* value of 72.1, 43.5 Å and 77.6, 44.9 Å, respectively, while the XRD pattern of **1b** and **1c** in the 2θ range of 3~10º didn't show distinct peaks (Fig. 2e). The distance values of the two peaks of **1b** and **1c** have a ratio of 1: $1/\sqrt{3}$, a structure characteristic of the hexagonal packing of molecules with the structure parameter of a = 83.3 Å for **1b** and a = 89.6 Å for **1c**.. These data are close to twice the length of the molecular distance for **1b** and **1c** in the extended configuration, respectively, indicating one molecule overlaps the other one in the process of self-assembly by the strong intermolecular hydrophobic interactions of cholesterols in **1b** and **1c**.

The self-assembly behaviour driven by water

Due to the amphiphilic characteristics of **1b** and **1c** (the existence of hydrophilic ethylene glycol chains and hydrophobic cholesterol), the self-assembly properties of the complexes as well as the chirality character may be regulated by the polarity of the solvent. Although the solubility of these complexes in water is poor, they can be soluble in ethanol at a concentration lower than 2.5×10^{-3} mol·L^{-1} for **1b** and 6.8×10^{-3} mol L^{-1} for **1c** after heating, and both of the complexes are soluble in THF in a large range of concentrations (Table 1). We studied the assembly properties of **1b** and **1c** in the mixed solvent of water/ethanol and water/THF, respectively. An interesting tuneable chirality was observed in the water/ethanol with a different solvent ratio.

1b or **1c** (1.0×10^{-4} mol·L^{-1}) can form a solution in a mix solvent of aqueous ethanol after heating the solution to 70 ºC and cooled to room temperature (20 ºC). The concentration of the samples is the same, while the volume percentage of water (r_{aq}) in the solvents varied in the different samples. The CD spectra of these samples were tested and are presented in Fig. 3 and Fig. S4 (in the ESI†). From the spectra, we could see that **1b** showed no obvious chiral signal in ethanol and the mixed solvents (Fig. S4 in the ESI†), indicating that **1b** could not self-assemble into macro helical structures under such conditions. This result is further confirmed by SEM (Figure S5 in the ESI†). The SEM image showed that **1b** formed spherical structures in pure ethanol. With the addition of water, the mixture of spherical and claviform appeared and aggregated to an irregular block structure (Fig. S5 in the ESI†). However, an interesting water-induced CD signal enhancement and reversal was observed in **1c** with longer ethylene glycol chains. **1c** shows a moderate positive Cotton effect at approximately 309 nm in pure ethanol. With the increase of the r_{aq}, the intensity of the CD signal increased first. When r_{aq} = 5%, the intensity of the CD signal became the strongest with the peak red shifted to 313 nm. However, with the continuous increase in the water ratio in the solvent, the intensity of the positive CD signal decreases and an opposite negative signal appears at approximately 300 nm when the r_{aq} = 22%. The intensity of the negative signal increases as r_{aq} < 25% and then decreases again and gradually disappears as r_{aq} increases to 50%. The above results indicate that the small amount of water in the mixed solvent can prompt the formation of the well-organized chiral ribbons; however, further addition of water overturns the chiral aggregation and finally damages the macro helix structure. Thus, water can behave as a trigger for helix aggregation, reversal and collapse in the self-assembly of **1c**. The above process was traced by SEM and TEM images.

Soft Matter Accepted Manuscript

This journal is © The Royal Society of Chemistry 2012

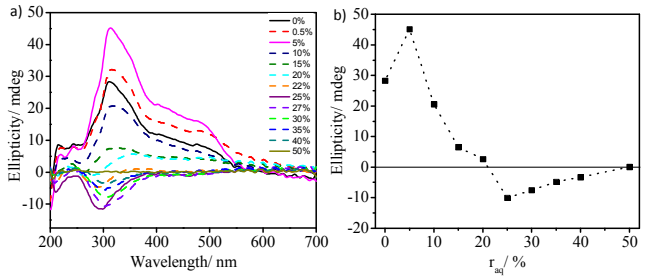

Fig. 3 a) The CD spectra of **1c** in water/ethanol with the increase of r_{aq}. b) The CD signal changes at 313 nm with the increase of r_{aq} in the mixed solvent. The concentration of all the samples is 1.0×10^{-4} mol·L^{-1}.

SEM images of **1c** in aqueous ethanol solution with different r_{aq} from 0% to 50% are measured and presented in Fig. 4. The SEM image of **1c** in pure ethanol shows short regular-sized helical claviform morphology with an average diameter of 300-500 nm and a length of 500-1000 nm (Fig. 4a). When r_{aq} = 2%, the left-handed helix became larger and clearer (Fig. 4b). When r_{aq} is approximately 5%, well-organized left-handed helical ribbons appeared (Fig. 4c). The screw-pitch and the width of the helix are approximately 600 and 500 nm, respectively, and the thickness of the helix ribbon is approximately 150 nm. The left-handed helical structure gradually became blurry as r_{aq} increased to 20% (Fig. 4d-4f). In contrast, when r_{aq} further increased to 25%, some right-handed chiral structure clearly appeared (Fig. 4g). The morphology of the self-assembled structure in Fig. 4g looks like a helical heterojunction. We can see the tendency of the change of the helical direction induced by water at this percentage. At an increase in r_{aq} to 30%, the right-handed helix (Fig. 4h, white arrow) became clearer with the coexistence of the left-handed helix (Fig. 4h, red arrow). This result indicates that the addition of water not only promotes the formation of helical structures but also affects the direction of the helical structures. With a further increase in r_{aq} to 50%, the right-handed structure disappears again and finally turns into vesicles with CD silence (Fig. 4k-l). The above morphology and chirality structural change is consistent with the CD spectra, which indicates that the right-handed helix is the mesophase from the left-handed helix to the vesicles.

Furthermore, TEM images were characterized for further information on the helical structure of **1c** in aqueous ethanol solutions (Fig. 5). The helical structure was clearly observed in the sample with a r_{aq} of 2% and 5% which is showed in Fig 4. When r_{aq} is 5%, the average helical pitch is approximately 400-600 nm, and the average width of the helix is approximately 500 nm, which is similar to the structure in the SEM images. From the edge of the ribbon, we can see that the helical ribbon contains several layers. On the other hand, the morphology of the self-assembled structure changes when the ratio of water increases. In this process, some vesicles appear with the helical ribbons as shown in Fig. 5c when the water percent rate is larger than 15%. When r_{aq} increases to 35%, both the left- and right-handed helical structures were observed (Fig. 5e). When the ratio of water increases to 50%, the helical structure turns into vesicles and the size of the vesicles becomes smaller (100-200 nm).

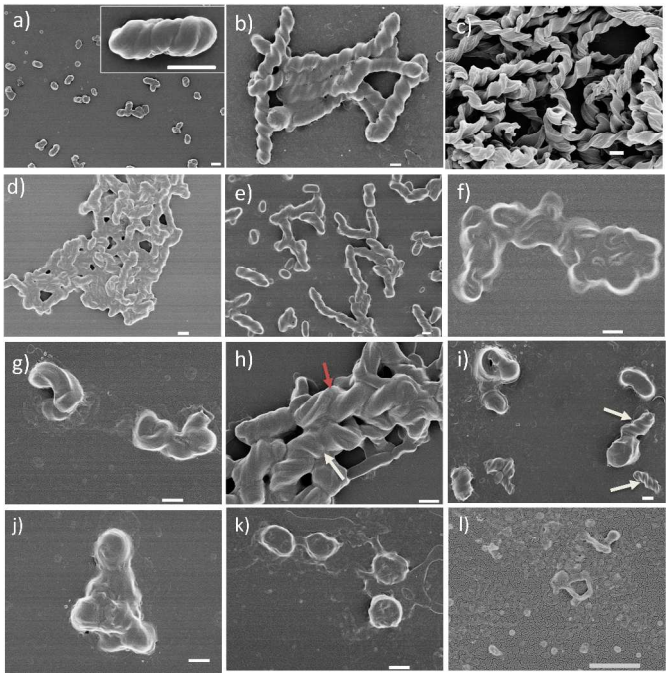

Fig 4 The SEM images of **1c** in water/ethanol with different r_{aq} of (a) 0%, (b) 2%, (c) 5%, (d) 10%, (e) 15%, (f) 20%, (g) 25%, (h) 30%, (i) 35%, (j) 40%, (k) 45%, (l) 50%. The scale bar of these images is 500 nm.

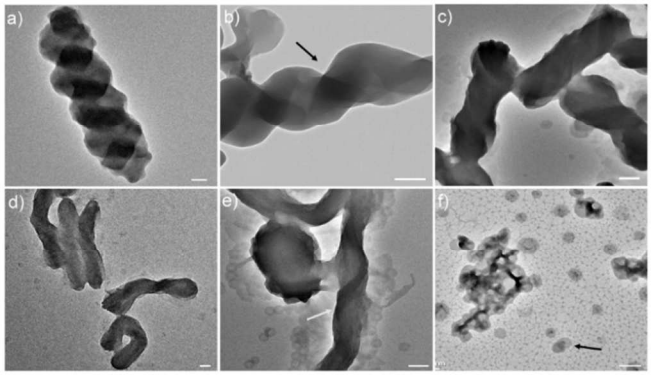

Fig. 5 The TEM images of 1c in which the percentage of water in the solvent is a) 0%, b) 5%, c) 10%, d) 15%, e) 35%, f) 50%. The scale bar of these images is 200 nm.

To ensure the samples taken from SEM and TEM are representative for all structures present in solution, dynamic light scattering (DLS) was performed on the solutions (Fig. 6 and Fig. S6). The DLS data for the aqueous ethanol solutions of **1c** with different r_{aq} revealed consistent results as shown in SEM and TEM images. The DLS of **1c** in pure ethanol (r_{aq} = 0) gave a broad size distribution between 200-800 nm with the average size of 370 nm, representing the nice dispersed helical claviform shown in Fig. 4a. Two size distributions of about 200 nm and 5 μm, respectively, in the DLS patterns were clearly seen in the r_{aq} range of 2% ≤ r_{aq}≤ 15%. The distribution of the larger size particles reaches to maximum when r_{aq} value was

Soft Matter Accepted Manuscript

5%. This is consistent with the liong helical structures shown in Fig. 4c. With further addition of water to the solvent, the number of big sized particles decreased again and disappeared when r_{aq} reaches to 25% and the average size of the particles further decreased to about 70 nm in the r_{aq} of 50% (Fig. S6). These data were also in agreement with the SEM images (Fig. 4i-4l).

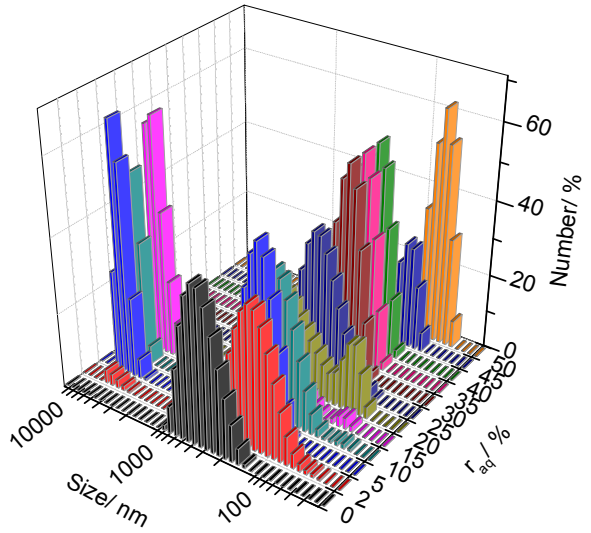

Fig. 6 The dynamic light scattering (DLS) of **1c** aqueous ethanol solution with different r_{aq} of 0%, 2%, 5%, 10%, 15%, 20%, 25%, 30%, 35%, 40%, 45% and 50%. Size distribution is by number.

The self-assembly properties of the complexes in other water-miscible solvents such as water/THF were also studied. All three complexes have nice solubility in THF. The diluted solution in water/THF with different ratios at the concentration of 1.0×10^{-4} mol·L^{-1} is tested via CD spectra and SEM. CD spectra showed that no clear chiral signal appeared in the water/THF solution of all of the complexes (Fig. S7 in the ESI†). This means that no helical structure formed in the process of self-assembly of **1a-1c** in the water/THF solution, which is confirmed by the SEM images (Fig. S8 in the ESI†). The SEM image of **1a** in the water/THF solvent shows spherical structures with a r_{aq} = 50% and irregular structures with the other ratios. Due to the large solubility difference of these complexes in THF and in water, samples may be supersaturated and quickly deposit in the process of solvent evaporation. It is obvious that the formation of helical structures depends on both the structure of the molecule and the property of the solvent.

The mechanism of the formation of the helical structure

To study the self-assembly process in the morphology evolution of **1c** in aqueous ethanol solution, the SAXS patterns of the solids from ethanol and water/ethanol with different volume ratio are characterized. The powder of **1c** precipitation in ethanol and water/ethanol is prepared via cooling the hot solution (4.0×10^{-3} mol L^{-1}) at room temperature. As the ratio of water increased, the precipitation that formed in the mixed solvent of water/ethanol presented different packing modes (Fig. 2f). The SAXS pattern and XRD diffraction of **1c** from pure ethanol had two peaks corresponding to the *d*-spacing of 43.7 and 21.6 Å (Fig. S9 in the ESI†) with a ratio of *d1/d2* = 1: 1/2, indicating a lamellar structure of **1c** in pure ethanol. The distance of 43.7 Å is close to the length of the molecule of **1c**, indicating that the lamellar structure is made by a mono layer. After an addition of water to a r_{aq} = 2%, this peak shifted slightly to a greater distance of 44.7 Å (Fig. 7a). When the r_{aq} was increased to 20%, the distance was further shifted to 46.7 Å and a new peak with a *d* value of approximately 76.1 Å was observed. The corresponding distances of these two peaks changed to 77.5 and 45.1 Å, with a value ratio of *d1/d2* = 1: $1/\sqrt{3}$, when the r_{aq} was 35%, indicating the hexagonal structure packing of the molecules with the structure parameter of *a* = 87.9 Å (Fig 7b). With the further increase in the r_{aq} up to 90%, the distances of the two peaks became 83.3 and 44.1 Å, with a value ratio approaching *d1/d2* = 1: 1/2 (Fig. 7c). The above data clearly show a structure transformation of **1c** from monolayer structures to bilayer structures with a mesophase of hexagonal structures in the process of water addition, accompanied by the transformation of the morphologies from the left helical ribbon structure to vesicles with a mesophase of right helical ribbon.

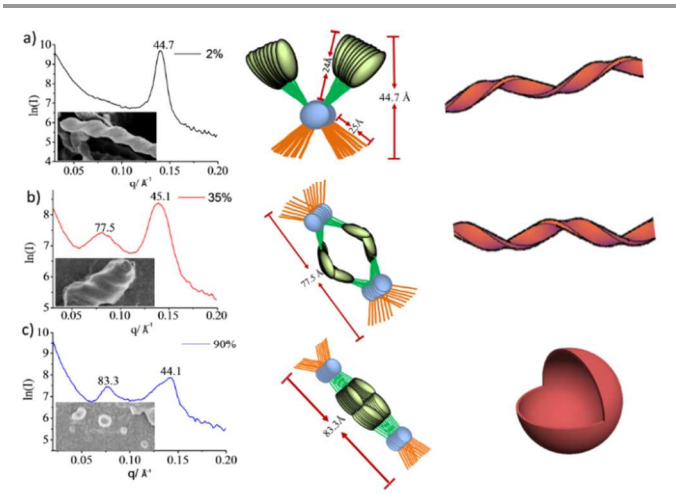

Fig. 7 The correlation of the SAXS pattern, SEM image and packing model of **1c** in water/ethanol with different r_{aq}.

A combination of the spectral and structural studies allows us to propose the mechanism of the observed morphological transitions of **1c** triggered by water. We observe three distinct morphologies in aqueous ethanol solutions with different percentages of water, namely the left-handed helix, right-handed helix and vesicles. We also observed some mixed mesophases such as helical heterojunction. There is a remarkable correlation between the morphology and the packing structure. It seems that the balance of the hydrophobic and hydrophilic effects plays a key role in the morphology and structural transition. The ethanol, as an amphiphilic solvent, produced an appropriate environment for **1c**; thus, **1c** favours the formation of monolayer lamellar aggregates by the balance of hydrophobic interactions between cholesterol moieties and

Soft Matter Accepted Manuscript

This journal is © The Royal Society of Chemistry 2012

the hydrophilic ether groups (Fig. 6). It is likely that the addition of water will cause the helical aggregates to assemble in such a way that the hydrophobic parts are shielded from the hydrophilic outside.[16] When small amounts of water were added (for example, to a r_{aq} <5%), the layer structure was not changed, but the helix formed a clearer shape. With a further increase in the r_{aq} (20%), the enhanced hydrophilicity of the solvent made the hydrophobic interaction of cholesterol moieties much stronger and provided a shield from the hydrophilic outside; therefore, **1c** packed as a bilayer hexagonal structure and changed the direction of the helix. The bilayer structure was also observed in the right-handed helical structure of the DMSO gel of **1a**. Finally, the bilayer structure of **1c** aggregated to the vesicles by hydrophobic interaction between cholesterol moieties with the hydrophilic ether groups posited at the surface of the vesicles. From the above study, we found that the change in the hydrophilicity of the solvent influences the packing mode of **1c** and is accompanied by morphological variations.

Conclusions

In summary, three alkynylplatinum (II) bipyridyl complexes with two cholesteric groups via alkyl chains and amido bonds are designed and synthesized. All of these complexes can self-assemble to gel networks in DMSO, while only the morphology of **1a** gel had a well-defined right-handed helical structure. In contrast, **1c**, with long ethers on the alkynyl fragment, can self-assemble into perfect left-handed helical structures in aqueous ethanol solutions with a specific volume percentage of water. In addition, three distinct morphologies, the left-handed helix, right-handed helix, and vesicles, as well as mixed mesophases such as helical heterojunction in aqueous ethanol solution with different percentages of water were observed. The correlation between the morphology and the packing structure was proposed. It seems that the balance of hydrophobic and hydrophilic effects plays a key role in the morphology and structural transition. This report clearly shows how the molecular self-assembly reacts to external effects and thus provides a strategy for the development of stimulus-responsive soft materials.

Acknowledgements

The authors thank for the financial support of the National Basic Research Program of China (2013CB733700), the China National Funds for Distinguished Young Scientists (21125104), National Natural Science Foundation of China (51373039), Specialized Research Fund for the Doctoral Program of Higher Education (20120071130008), Program for Innovative Research Team in University (IRT1117), Program of Shanghai Subject Chief Scientist (12XD1405900), and Shanghai Leading Academic Discipline Project (B108).

Notes and references

a Department of Chemistry and Concerted Innovation Center of Chemistry for Energy Materials, Fudan University, 220 Handan Road, Shanghai 200433 (China), Fax: (+86) 21-55664621, E-mail: yitao@fudan.edu.cn

† Electronic Supplementary Information (ESI) available: Synthesis and characterizations of complexes, SAXS, XRD, CD, SEM images. See DOI: 10.1039/b000000x/

1 E. Yashima, K. Maeda, H. Iida, Y. Furusho and K. Nagai, *Chem. Rev.*, 2009, **109**, 6102-6211.
2 R. J. Mart, R. D. Osborne, M. M. Stevens and R. V. Ulijn, *Soft Matter*, 2006, **2**, 822-835.
3 L. C. Palmer, Y. S. Velichko, M. O. de la Cruz and S. I. Stupp, *Philosophical Transactions of the Royal Society A: Mathematical, Physical and Engineering Sciences*, 2007, **365**, 1417-1433.
4 K. Nagai, K. Maeda, Y. Takeyama, T. Sato and E. Yashima, *Chem.-Asian J.,* 2007, **2**, 1314-1321.
5 M. M. J. Smulders, I. A. W. Filot, J. M. A. Leenders, P. van der Schoot, A. R. A. Palmans, A. P. H. J. Schenning and E. W. Meijer, *J. Am. Chem. Soc.*, 2010, **132**, 611-619.
6 A. Gopal, M. Hifsudheen, S. Furumi, M. Takeuchi and A. Ajayaghosh, *Angew. Chem.*, 2012, **124**, 10657-10661.
7 C. T. Chen, C.-H. Chen and T. G. Ong, *J. Am. Chem. Soc.*, 2013, **135**, 5294-5297.
8 Q. Li, L. Green, N. Venkataraman, I. Shiyanovskaya, A. Khan, A. Urbas and J. W. Doane, *J. Am. Chem. Soc.*, 2007, **129**, 12908-12909.
9 R. Sun, C. Xue, X. Ma, M. Gao, H. Tian and Q. Li, *J. Am. Chem. Soc.*, 2013, **135**, 5990-5993.
10 T. Muraoka, H. Cui and S. I. Stupp, *J. Am. Chem. Soc.*, 2008, **130**, 2946-2947.
11 S. Sakurai, K. Okoshi, J. Kumaki and E. Yashima, *J. Am. Chem. Soc.*, 2006, **128**, 5650-5651.
12 R. S. Johnson, T. Yamazaki, A. Kovalenko and H. Fenniri, *J. Am. Chem. Soc.*, 2007, **129**, 5735-5743.
13 H. Goto, Y. Okamoto and E. Yashima, *Macromolecules*, 2002, **35**, 4590-4601.
14 Y. Huang, J. Hu, W. Kuang, Z. Wei and C. F. J. Faul, *Chem. Commun.*, 2011, **47**, 5554-5556.
15 P. A. Korevaar, C. Schaefer, T. F. A. de Greef and E. W. Meijer, *J. Am. Chem. Soc.*, 2012, **134**, 13482-13491.
16 M. A. J. Gillissen, M. M. E. Koenigs, J. J. H. Spiering, J. A. J. M. Vekemans, A. R. A. Palmans, I. K. Voets and E. W. Meijer, *J. Am. Chem. Soc.*, 2014, **136**, 336-343.
17 S. J. George, Z. Tomovic, A. P. H. J. Schenning and E. W. Meijer, *Chem. Commun.*, 2011, **47**, 3451-3453.
18 H. Cao, X. Zhu and M. Liu, *Angew. Chem. Int. Ed.*, 2013, **52**, 4122-4126.
19 Y. Yan, K. Deng, Z. Yu and Z. Wei, *Angew. Chem. Int. Ed.*, 2009, **48**, 2003-2006.
20 Y. Yan, Z. Yu, Y. W. Huang, W. X. Yuan and Z. X. Wei, *Adv. Mater.*, 2007, **19**, 3353-3357.
21 T. Tazawa, S. Yagai, Y. Kikkawa, T. Karatsu, A. Kitamura and A. Ajayaghosh, *Chem. Commun.*, 2010, **46**, 1076-1078.
22 K. P. Divya, S. Sreejith, C. H. Suresh and A. Ajayaghosh, *Chem. Commun.*, 2010, **46**, 8392-8394.

Soft Matter Accepted Manuscript

23 S. J. George, R. de Bruijn, Z. Tomovic, B. Van Averbeke, D. Beljonne, R. Lazzaroni, A. P. H. J. Schenning and E. W. Meijer, *J. Am. Chem. Soc.*, 2012, **134**, 17789-17796.
24 X. Wang, G. Guerin, H. Wang, Y. Wang, I. Manners and M. A. Winnik, *Science*, 2007, **317**, 644-647.
25 P. Besenius, G. Portale, P. H. H. Bomans, H. M. Janssen, A. R. A. Palmans and E. W. Meijer, *PNAS*, 2010, **107**, 17888-17893.
26 M. Wolffs, J. L. J. van Velthoven, X. Lou, R. A. A. Bovee, M. Pouderoijen, J. L. J. van Dongen, A. P. H. J. Schenning and E. W. Meijer, *Chem.-.Eur. J.*, 2012, **18**, 15057-15064.
27 F. Helmich, C. C. Lee, A. P. H. J. Schenning and E. W. Meijer, *J. Am. Chem. Soc.*, 2010, **132**, 16753-16755.
28 S. Cantekin, D. W. R. Balkenende, M. M. J. Smulders, A. R. A. Palmans and E. W. Meijer, *Nature Chemistry*, 2011, **3**, 42-46.
29 Y. Yan, J. Fang, J. Liang, Y. Zhang and Z. Wei, *Chem. Commun.*, 2012, **48**, 2843-2845.
30 S. Kawano, N. Fujita and S. Shinkai, *J. Am. Chem. Soc.*, 2004, **126**, 8592-8593.
31 K. Murata, M. Aoki, T. Suzuki, T. Harada, H. Kawabata, T. Komori, F. Ohseto, K. Ueda and S. Shinkai, *J. Am. Chem. Soc.*, 1994, **116**, 6664-6676.
32 K. Liu, L. Meng, S. Mo, M. Zhang, Y. Mao, X. Cao, C. Huang and T. Yi, *J. Mater. Chem. C*, 2013, **1**, 1753-1762.
33 X. Yu, Q. Liu, J. Wu, M. Zhang, X. Cao, S. Zhang, Q. Wang, L. Chen and T. Yi, *Chem. –Eur. J.*, 2010, **16**, 9099-9106.
34 M. Zhang, S. Sun, X. Yu, X. Cao, Y. Zou and T. Yi, *Chem. Commun.*, 2010, **46**, 3553-3555.
35 M. Zhang, B. Wang, T. Jiang, M. Jiang and T. Yi, *CrystEngComm*, 2012, **14**, 8057-8062.
36 M. Zhang, L. Meng, X. Cao, M. Jiang and T. Yi, *Soft Matter*, 2012, **8**, 4494-4498.
37 M. Zhang, M. Jiang, L. Meng, K. Liu, Y. Mao and T. Yi, *Soft Matter*, 2013, **9**, 9449-9454.
38 S. Shinkai and K. Murata, *J. Mater. Chem.*, 1998, **8**, 485-495.
39 K. Murata, M. Aoki and S. Shinkai, *Chem. Lett.*, 1992, 739-742.
40 P. Terech, E. Ostuni and R. Weiss, *J. Phys. Chem.*, 1996, **100**, 3759-3766.
41 R. Wang, C. Geiger, L. Chen, B. Swanson and D. G. Whitten, *J. Am. Chem. Soc.*, 2000, **122**, 2399-2400.
42 J. H. Jung, Y. Ono, K. Hanabusa and S. Shinkai, *J. Am. Chem. Soc.*, 2000, **122**, 5008-5009.
43 T. Ishi-i, Y. Ono and S. Shinkai, *Chem. Lett.*, 2000, **29**, 808-809.
44 J. Wu, T. Yi, T. Shu, M. Yu, Z. Zhou, M. Xu, Y. Zhou, H. Zhang, J. Han, F. Li and C. Huang, *Angew. Chem.*, 2008, **120**, 1079-1083.
45 J. Wu, T. Yi, Q. Xia, Y. Zou, F. Liu, J. Dong, T. Shu, F. Li and C. Huang, *Chem. –Eur. J.*, 2009, **15**, 6234-6243.
46 J. Wang, Y. Chen, Y.-C. Law, M. Li, M.-X. Zhu, W. Lu, S. S.-Y. Chui, N. Zhu and C.-M. Che, *Chem. – Asian J.*, 2011, **6**, 3011-3019.
47 W. Lu, K.-M. Ng and C.-M. Che, *Chem. – Asian J.*, 2009, **4**, 830-834.
48 A. Y. Y. Tam, K. M. C. Wong and V. W. W. Yam, *J. Am. Chem. Soc.*, 2009, **131**, 6253-6260.
49 A. Y. Y. Tam, K. M. C. Wong and V. W. W. Yam, *Chem. – Eur. J.*, 2009, **15**, 4775-4778.
50 A. Y. Tam, K. C. Wong, N. Zhu, G. Wang and V. W. Yam, *Langmuir*, 2009, **25**, 8685-8695.
51 A. Y. Y. Tam, K. M. C. Wong, G. Wang and V. W. W. Yam, *Chem. Commun.*, 2007, **20**, 2028-2030.
52 I. Maity, D. B. Rasale and A. K. Das, Soft Matter, 2012, **8**, 5301-5308.
53 X. Wang and Z. Guo, *Chem. Soc. Rev.*, 2013, **42**, 202-224.
54 M. C. L. Yeung and V. W. W. Yam, *Chemical Science*, 2013, **4**, 2928-2935.
55 M. O. M. Piepenbrock, G. O. Lloyd, N. Clarke and J. W. Steed, *Chem. Rev.*, 2009, **110**, 1960-2004.
56 Y. Li, A. Y. Y. Tam, K. M. C. Wong, W. Li, L. Wu and V. W. W. Yam, *Chem. – Eur. J.,* 2011, **17**, 8048-8059.

Soft Matter Accepted Manuscript

 This journal is © The Royal Society of Chemistry 2012

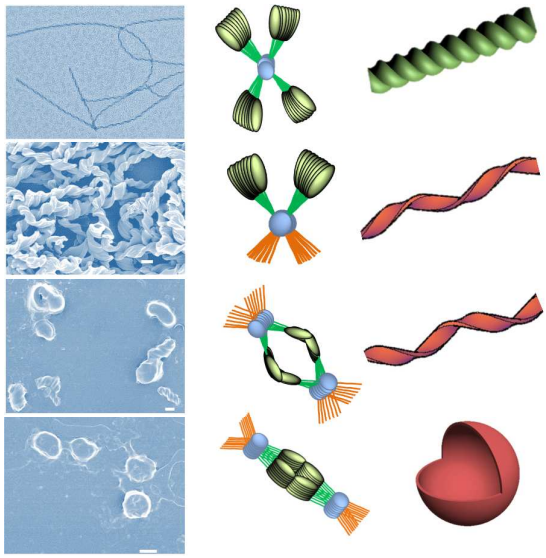

The gelation and solvent triggered helical aggregations were reported in the self-assembly of cholesterol tailed platinum complexes

Soft Matter Accepted Manuscript